ISSN1027-5495. Functional Materials, 30, No.4 (2023), p. 494-505
doi:http://dx.doi.org/10.15407/fm30.04.494

4`-Benzyloxyflavonol glucoside as fluorescent indicator for β-glucosidase activity

L.V. Chepeleva,[1] D.O. Tarasenko,[1] A.Y. Chumak,[1] O.O. Demidov,[1] A.D. Snizhko,[1] O.O. Kolomoitsev,[1] V.M. Kotliar,[1] E.S. Gladkov,[1,2] A.L. Tatarets,[2] A.V. Kyrychenko[1,2], A. D. Roshal[1,*]

[1]Institute of Chemistry and School of Chemistry, V. N. Karazin Kharkiv National University, 4 Svobody Sq., Kharkiv 61022, Ukraine.
[2]State Scientific Institution ''Institute for Single Crystals'', National Academy of Sciences of Ukraine, 60 Nauky Ave., Kharkiv 61072, Ukraine.

Received September 25,2023

Fluorescent flavonols and their glucosylated derivatives are promising tools for studying protein structure and enzyme activity screening. The fluorescence properties of such probes are tunable by electron-withdrawing substituents in 2-aryl ring, while a role of bulky hydrophobic groups has not been examined in-depth yet. Here, we examine the application of benzyloxy-substituted flavonol ß-D-glucoside as a fluorescent indicator for the activity screening of the ß-glucosidase enzyme in an aqueous solution. The rate constant of the enzymatic cleavage of an O-glycosidic bond in benzyloxy-substituted and un-substituted flavonol glucosides was compared using fluorescence kinetic measurements. We found that introducing a hydrophobic bulky benzyloxy group in the 4`-position of flavonol glucoside resulted in a 2.3-fold decrease in the hydrolysis rate constant. The molecular docking calculations allowed us to reveal critical molecular interactions in a flavonol-enzyme complex and identify favorable binding modes and the binding affinity of the flavonols towards the ß-glucosidase protein. We found that upon adding a bulky benzyloxy group, the flavonol glucoside's binding affinity towards the enzyme was increased from -9.9 to -10.8 kcal/mole. However, the stronger binding of the substituted glucoside would require a higher activation energy barrier to form an appropriate substrate-receptor transition state for the hydrolysis reaction, seen as some decrease in the rate constant. Finally, these findings promise that flavonol glucosides can be utilized as easy-to-use fluorescent indicators for rapid activity screening of other enzymes from a glucosidase family.

Keywords: flavonol, fluorescence probe, ß-glucosidase, glycosidic bond cleavage, fluorescence indicator, molecular docking

Бензилокси-заміщений флавонол гликозид як флуоресцентний індикатор для активності β-глюкозидази. *Л.В. Чепелева, Д.О. Тарасенко, А.Ю. Чумак, О.О. Демидов, А.Д. Сніжко, О.О. Коломойцев, В.М. Котляр, Е.С. Гладков, А.Л. Татарець, О.В. Кириченко, О. Д. Рошаль*

Флуоресцентні флавоноли та їх глюкозильовані похідні є перспективними для вивчення структури білка та скринінгу активності ферментів. Флуоресцентні властивості таких зондів регулюються електроно-акцепторними замісниками у 2-арильному кільці, тоді як роль об'емних гідрофобних груп ще не достатньо вивчена. В цій роботі ми вивчаємо застосування бензилокси-заміщеного флавонол ß-D-глюкозиду, як флуоресцентного індикатора для перевірки активності ферменту ß-глюкозидази у водному розчині. Константу швидкості ферментативного розщеплення О-глікозидного зв'язку в бензилоксизаміщених і незаміщених флавонолах-індикаторах порівнювали за допомогою кінетичних вимірювань флуоресценції. Показано, що введення гідрофобної об'емної бензилоксигрупи у 4`-

положення флавонол глюкозиду призводило до 2,3-кратного зниження константи швидкості гідролізу. Розрахунки молекулярного докінгу дозволили виявити критичні молекулярні взаємодії в комплексі флавонол-фермент і визначити вигідну конформацію та афінність зв'язування флавонолів з білком ß-глюкозидази. Встановлено, що після додавання об'ємної бензилоксигрупи афінність зв'язування глюкозиду флавонолу з ферментом збільшувалася з -9,9 до -10,8 ккал/моль. Однак більш міцне зв'язування заміщеного глюкозиду вимагало б більш високого енергетичного бар'єру активації для формування відповідного перехідного стану для реакції гідролізу у комплексі субстрат-рецептор, що може призводити до зниження константи швидкості. Результати роботи показують, що глюкозиди флавонолу можна використовувати як прості у використанні флуоресцентні індикатори для швидкого скринінгу активності інших ферментів із сімейства глюкозидаз.

1. Introduction

Flavonol-based fluorescent probes represent a class of environmentally sensitive dyes whose emission properties are highly sensitive to their immediate environment [1-9]. Their notable feature is the excited-state intramolecular proton transfer (ESIPT) phenomenon [10-11]. A proton transfer reaction occurs through an intramolecular hydrogen bond bridge between an adjacent hydroxyl group and carbonyl oxygen atom in a flavonoid moiety, resulting in an extremely fast ($k_{ESIPT} > 10^{12}$ s^{-1}) phototautomerization. ESIPT occurs from a normal form (N*) to a tautomeric one (T*) [7, 12-13], resulting in the appearance of the dual-wavelength emission (Figure 1), which allows the ratiometric fluorescence detection [1, 12].

Among many promising applications, flavonols have been used as solvatochromogenic probes for monitoring solvent polarity [1, 14-15] and pH changes [16-17], as well as monitoring water impurities in organic solvents [18]. Moreover, flavonol derivatives have demonstrated outstanding selectivity for certain metal ions in solution [7, 17, 19-22]. Unique fluorescent properties in combination with good biocompatibility makes flavonols as a biomolecular probe for protein structure and dynamic [23]. Upon tight binding to proteins, such as lysozymes [24] and human albumins, flavonols demonstrate an essential fluorescence "turn-on" effect [19, 23], opening up the opportunity for monitoring inner protein structure and folding [9, 23, 25].

It has recently been demonstrated that 4`-fuoroflavonol ß-D-glucoside can be used as a fluorescent indicator of ß-glucosidase activity [26-27] (Figure 1). ß-Glucosidases are a group of enzymes, which catalyze the hydrolysis of cellobiose, aryl and alkyl ß-D-glucoside. ß-glucosidase are widely spread in nature, they are present in plants, fungi, animals, bacteria and yeast also contained in the soil. In addition, ß-glucosidases have been used in various biotechnological processes, such as biofuel production and oligosaccharide synthesis. The role of ß-glucosidases, contained in the soil, is extremely important, since they take part in the catalytic hydrolysis and biodegradation of various ß-glycosides in plants. In addition, the activity and concentration of glucosidase is a measure of soil quality [28]. The important role of ß-glucosidase in various aspects of plant physiology has been reported [29]; for example, it initiates chemical protection against pathogens [30]. Regula-

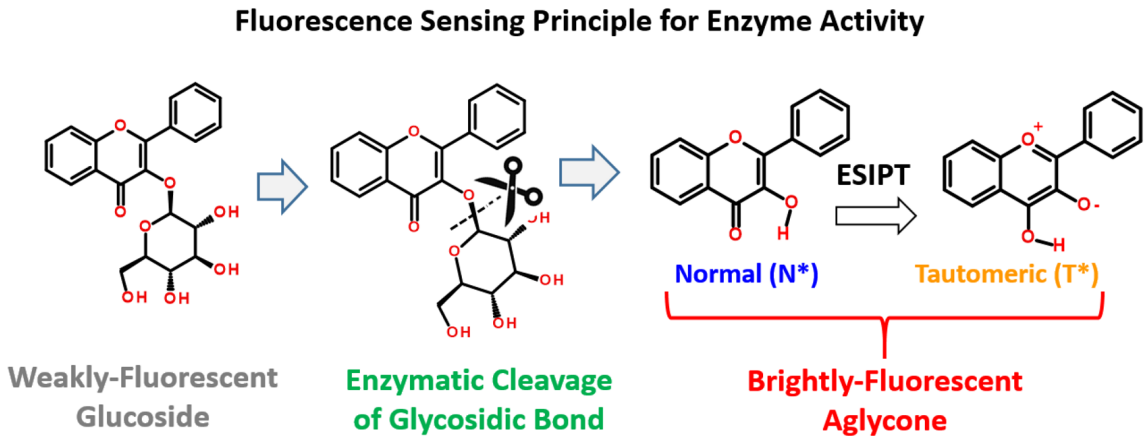

Fig. 1. Scheme of a fluorescence sensing principle of the enzyme activity using a flavonol-glucoside indicator.

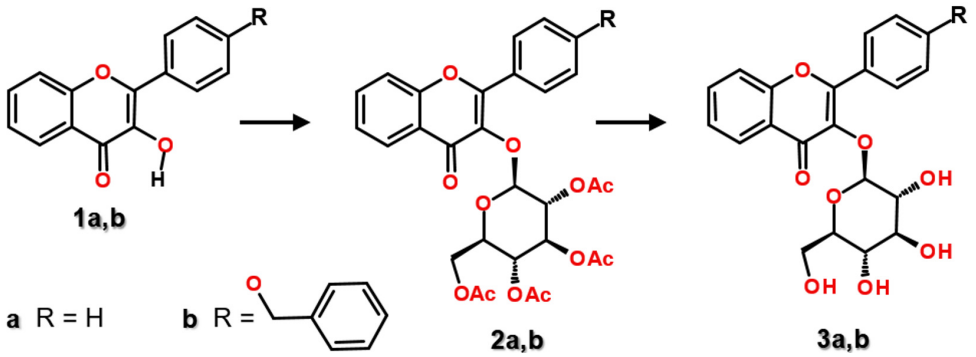

Scheme 1. Synthesis of flavonol ß-D-glucosides **3a-b**.

tion of glucosidase activity affects the course of Gaucher's disease [31], as well as the effectiveness of chemotherapy for breast cancer [32].

In this work, we study the application of benzyloxy-substituted flavonol ß-D-glucoside as a fluorescent indicator for the activity screening of the ß-glucosidase enzyme. First, fluorescence kinetic measurements were used to evaluate the rate constant of the enzymatic cleavage of an O-glycosidic bond in benzyloxy-substituted and un-substituted flavonol glucosides. Second, critical molecular interactions in a flavonol-enzyme complex and favorable binding modes of the studied glucosides were examined by molecular docking calculations Finally, the perspective for applying flavonol glucosides as fluorescent indicators for rapid activity screening of other glucosidases is discussed.

2. Experimental

Materials and Methods. ^{1}H and ^{13}C NMR spectra (400 and 100 MHz) were recorded on Bruker Avance 400 and Varian MR-400 spectrometers in DMSO-d_6. ^{1}H and ^{13}C chemical shifts were reported relative to residual protons and the carbon atoms of the solvent (2.49 and 39.5 ppm, respectively) as the internal standard. The LCMS spectra were recorded using a chromatography/mass spectrometric system that consists of a high-performance liquid chromatography Agilent 1100 Series equipped with a diode matrix and a mass selective detector Agilent LC/MSD SL, column SUPELCO Ascentis Express C18 2.7 µm 4.6 mm × 15 cm. Elemental analysis was realized on a EuroVector EA-3000 instrument. TLC was performed using Polychrom SI F254 plates. Melting points of all synthesized compounds were determined with a Hanon Instruments automatic melting point apparatus MP450 in open capillary tubes.

According to the HPLC MS data, all synthesized compounds are >95% pure. All solvents and reagents were commercial grade and, if required, purified in accordance with the standard procedures. Starting unsaturated ketones were synthesized as described in [33].

ß-Glucosidase (ß-D-glucoside glucohydrolase) from Almonds were purchased from Sigma-Aldrich as lyophilized powder with > 98% purity.

Flavonol synthesis. The synthesis of 2-aryl-3-hydroxy-4H-chromen-4-ones (flavonols) is well known and described elsewhere. The general procedures of syntheses of most typical substances of the series used in our work and typical examples of substance characteristics are given in the experimental section.

Synthesis of Flavonol Glucosides. Syntheses of flavonol glucosides (**3a**, **3b**) were performed using the corresponding flavonol aglycones **1a-b**. The glucosylation was made according to a modified method described by Scheme 1 [34].

A tetraacetyl glucoside of unsubstituted flavonol **2a** has been obtained using the following procedure. 100 mg (0.4 mmol) of 2-aryl-3-hydroxy-4H-chromen-4-one (flavonol) (**1a**) and 172 mg (0.4 mmol) 2,3,4,6-O-tetraacetyl-α-glucopyranosyl bromide were dissolved in 5 ml dimethylformamide, and under stirring, 120 mg (0.8 mmol) of K_2CO_3 were added. The mixture was stirred in the argon atmosphere for 48 h at 80ºC. Then the solvent was evaporated under low pressure, and the residue obtained was dissolved in ethyl acetate. The organic phase was washed by water, dried with anhydrous Na_2SO_4, and the solvent was evaporated again. The obtained intermediate product was purified by column gradient chromatography using an ethylacetate-hexane eluent with a composition varying from 0:100 to 60:40. The yellow crys-

tals were obtained with a yield of 62 mg (26%). Physico-chemical parameters of the compound are: t_m – 175-177 °C, $C_{30}H_{30}O_{11}$, ^{1}H NMR (500 MHz, $CDCl_3$) δ 8.23 (d, J = 8.1 Hz, 1H), 8.05 (d, J = 5.3 Hz, 2H), 7.69 (t, J = 7.7 Hz, 1H), 7.54 (d, J = 8.5 Hz, 1H), 7.49 (d, J = 2.4 Hz, 3H), 7.42 (t, J = 7.6 Hz, 1H), 5.70 (d, J = 7.8 Hz, 1H), 5.33 – 5.23 (m, 1H), 5.22 – 5.15 (m, 1H), 5.06 (t, J = 9.7 Hz, 1H), 4.03 – 3.89 (m, 2H), 3.61 (d, J = 10.4 Hz, 1H), 2.09 (s, 3H), 2.00 (s, 3H), 1.98 (s, 3H), 1.87 (s, 3H). ^{13}C NMR (126 MHz, DMSO-d_6) δ 175.6, 171.1, 170.6, 170.4, 169.4, 161.1, 158.4, 154.5, 134.4, 134.2, 130.6, 127.0, 124.1, 123.0, 122.4, 118.3, 115.1, 97.5, 70.3, 69.9, 69.4, 67.3, 61.9, 20.7, 20.6. Mass spectrum, m/z (I_{rel}, %): 569 (100), 331(29).

A tetraacetyl glucoside of 4'-benzyloxy flavonol **2b** was obtained by the same procedure. Mass spectrum of **2b**: m/z($M+H^+$) is 675 (100%).

Deacetylation of flavonol tetraacetyl glucoside **2a** was carried out as follows: 56.8 mg (0.1 mmol) of tetraacetyl glucoside of unsubstituted flavonol (2) was dissolved in 5 ml of methanol, then 10 mg (~ 0.1 mmol) of sodium buthanolate was added, and the obtained mixture was stirred for 12 hours at room temperature. Then the mixture was diluted 2 times with water and neutralized by a diluted aqueous solution of HCl. Methanol was further evaporated from water solution under low pressure, and then, the target glucoside was extracted with ethyl acetate. The organic extract was dried, and then the solvent was evaporated. Physico-chemical parameters of the compound are: t_m – 185-186 °C, ^{1}H NMR (400 MHz, DMSO-d_6) δ 8.16 (s, 2H), 8.10 (s, 1H), 7.83 (s, 1H), 7.79 – 7.71 (m, 1H), 7.54 (dd, J = 236.5, 5.2 Hz, 4H), 5.58 (d, J = 7.2 Hz, 1H), 5.39 (d, J = 4.8 Hz, 1H), 5.06 (d, J = 5.0 Hz, 1H), 4.95 (s, 1H), 4.27 (s, 1H), 3.53 (s, 1H), 3.34 (s, 1H), 3.22 (s, 1H), 3.14 (s, 1H), 3.07 (s, 2H). ^{13}C NMR (126 MHz, DMSO-d_6) δ 173.5, 155.6, 154.7, 136.2, 134.1, 130.6, 129.0, 128.1, 125.1, 125.0, 123.2, 100.4, 77.4, 76.4, 74.0, 69.8, 60.7. Mass spectrum, m/z (I_{rel}, %): 401(100).

4'-Benzyloxy-flavonol glucoside **3b** was synthesized by the same procedure.

Spectral data of **3b**: ^{1}H NMR (400 MHz, DMSO-d6) δ 8.19 (d, J = 8.6 Hz, 2H), 8.09 (d, J = 7.7 Hz, 1H), 7.81 (d, J = 7.7 Hz, 1H), 7.74 (d, J = 8.3 Hz, 2H), 7.51-7.46 (m, 4H), 7.45-7.32 (m, 2H), 7.17 (d, J = 8.8 Hz, 2H), 5.57 (d, J = 7.5 Hz, 1H), 5.42 (d, J = 4.3 Hz, 1H), 5.22 (s, 2H), 5.07 (d, J = 4.7 Hz, 1H), 4.96 (s, 1H), 4.27 (s, 1H), 3.64 – 3.47 (m, 1H), 3.28 – 3.13 (m, 2H), 3.08 (s, 2H), 1.24 (d, J = 9.5 Hz, 2H). In mass spectra, a peak m/z($M+H^+$) 507(100) was detected.

Enzyme Activity Screening using Fluorescent Indicators. Kinetic studies of enzymatic hydrolysis of probes **3a-b** are measured after mixing two separate stock solutions of a flavonol glucoside and the ß-glucosidase enzyme. Mixing the subsequent stocks triggers probe-enzyme binding, upon which the O-glycosidic bond cleavage in probes **3a-b** occurs.

A stock solution of a flavonol glucoside was prepared by dissolving its sample in DMSO. A stock solution of ß-glucosidase was prepared by dissolving a sample of the enzyme in an aqueous phosphate buffer with pH 6.86. Next, the aliquots of both solutions were transferred to 1 ml of a buffer solution (pH 6.86), and the obtained mixture was further used for kinetic studies. The volumes of the aliquots of both stock solutions were chosen so that the final mixture contained similar concentrations of a flavonol glucoside and the ß-glucosidase enzyme, ranging from 5.0 to 7.0×10^{-5} mol/L.

The enzymatic hydrolysis reaction was carried out while stirring the mixture at a constant temperature. During the hydrolysis process, aliquots of 0.1 ml were taken at 1, 2, 6, 10, 15, and 30 min after the start of the reaction. Immediately after sampling, each aliquot was transferred to 2.5 ml of dichloromethane and intensively shaken. Using extraction, a mixture of the original flavone glycoside and its hydrolysis derivative – a flavonol aglycone, was separated from the enzyme. Next, the fluorescence spectra of the mixture of the glycoside and aglycone were recorded in the organic phase.

The fluorescence was excited at 360 nm, in the range of glucoside and aglycone absorption. The fluorescence spectra were recorded in the range of 380-600 nm. The emission intensity (I_F) at the maximum of the long-wavelength fluorescence band, in the range of 510-540 nm depending on flavonol structure, was used as quantitative parameter for kinetics studies.

The value of I_F, which is proportional to the aglycone concentration and inversely proportional to the glucoside concentration ($C_{\text{glucoside}}$) in the reaction mixture, was converted to $C_{\text{glucoside}}$ and then used to determine the reaction order and calculate the rate constant of enzymatic hydrolysis.

All the reagents and solvents were commercial and were used without additional purification.

Spectroscopic measurements. Absorption spectra were recorded by an Agilent Cary 3500 UV-Vis Multicell Spectrophotometer. Fluorescence was measured using a Hitachi 850 steady-state fluorescence spectrometer equipped with double-grating excitation and emission monochromators and a Cary Eclipse (Varian) fluorescence spectrometer. The fluorescence measurements were made in the buffer pH 6.86 (100 mM) in a 10×10 mm cuvette maintained at 20 ºC.

Molecular docking setup. The preparation of the receptor and ligands were carried out with the AutoDock Tools (ADT) software, version 1.5.7 [35]. The addition of hydrogen, the calculation of the Gasteiger charges of the receptor, and ligands were also performed using the ADT software. Molecular docking calculations were performed with the AutoDock Vina 1.1.2 software [36]. The 3D X-ray structure of *Paenibacillus polymyxa* ß-glucosidase B (BglB, PDB ID: 2O9R) [37] was downloaded from the RCSB Protein Data Bank.

We carried out the semi-flexible docking, so that the receptor was kept rigid and the ligand molecules were conformational flexible. The size of the cubic box generated by the ADT software, in the region of the receptor interaction (residues Glu167 and Glu356 for bBG was defined as 65×65×65 Å. The center of the grid box was set at Cartesian coordinates x=61.980, y=31.109 and z=40.606 with the grid point spacing set to 0.375 Å, respectively. For all runs, the number of binding modes was set to 9 and the exhaustiveness to 64. For each ligand, three independent runs were performed using different random seeds. The best docking mode corresponds to the largest ligand-binding affinity. Molecular graphics and visualization were performed using VMD 1.9.3 [38].

3. Results and discussion

Fluorescence Measurements of β-Glucosidase Activity

Glucosides of unsubstituted flavonol **3a** and 4'-benzyloxyflavonol **3b** were selected as fluorescent probes for ß-glucosidase activity because they and their aglycones have different fluorescent properties.

As mentioned above, a very important phenomenon, determining fluorescent properties of flavonol aglycones, is the ability to undergo intramolecular proton transfer in the excited state (ESIPT), which leads to the formation of a phototautomer (Figure 1). The tautomeric form of aglycones emits intense fluorescence in the green-yellow range of a spectrum, avoiding spectral overlap with other blue-emitting species [13]. The key conditions necessary for the ESIPT process to occur are the high excited-state basicity of the carbonyl group and the acidity of the 3-hydroxy group, as well as the presence of a hydrogen bond bridging these two groups [8, 13, 39].

The unsubstituted flavonol aglycone **1a**, in its initial excited N* state, does not exhibit fluorescence in aprotic solvents due to the faster rate of proton transfer compared to the emission rate [13]. Consequently, only the emission band of the phototautomer is observable in the fluorescence spectra. In protic solvents, the intramolecular hydrogen bond is either partially or entirely broken due to the formation of intermolecular hydrogen bonds with solvent molecules, so that a weak fluorescence from the N* form can be found [7-8, 39]. A weak intensity of the N* emission can be attributed to the pronounced intersystem crossing, a result of the small energy gap between the lowest excited states of the ππ* and nπ* types. When the unsubstituted flavonol aglycone **1a** directly interacts with ß-glucosidase, it enters the enzyme's active site, which is less polar and hydrophilic than the aqueous medium [40]. That promotes the formation of flavonol molecules with intramolecular hydrogen bonds, leading to an increase in phototautomer fluorescence.

In flavonol glycoside **3a**, the hydrogen atom of the 3-hydroxy group is substituted by a glucopyranoside moiety making ESIPT impossible. Thus, the fluorescent properties of **3a** in aqueous solutions, in complex with ß-glucosidase or in non-polar solvents must be similar to the N* fluorescence of **1a**. As a result, the following spectral effects might be expected: the hydrolysis of **3a** by the ß-glucosidase enzyme and the formation of **1a** in aqueous medium will not lead to changes in the fluorescence spectra. A very weak fluorescence of N* in an aqueous medium can be observed both before and after the hydrolysis. When performing the extraction of **3a** into the organic medium before the hydrolysis, the fluorescence properties of the organic phase will correspond to those of the aqueous one. When making the extraction after the hydrolysis, the organic phase will demonstrate a bright fluorescence of **1a** phototautomer. Thus, the appearance of T* fluorescence in the organic phase after incubation of **3a** with the enzyme

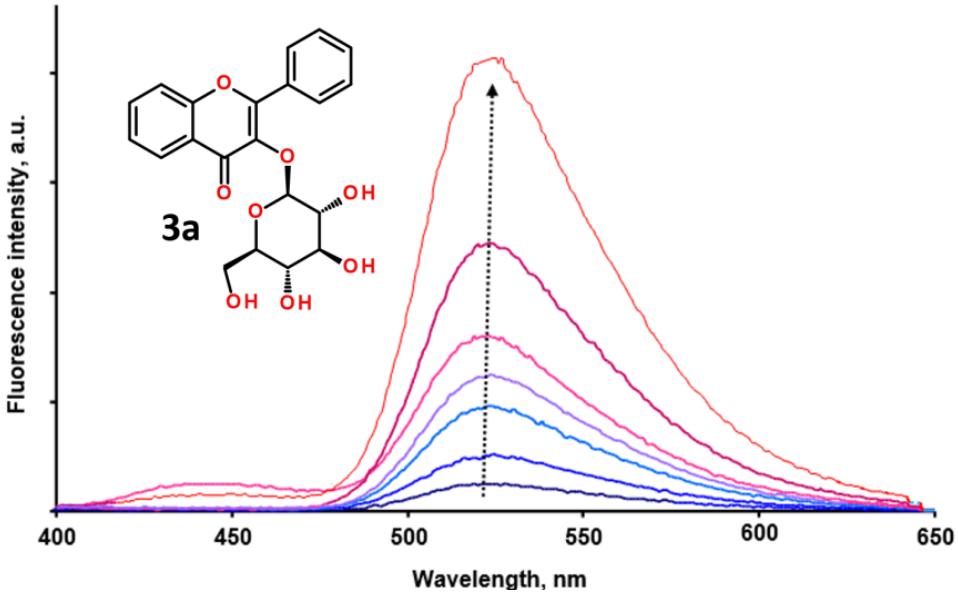

Fig. 2. Changes of fluorescent spectra during the hydrolysis reaction in the system probe **3a** – ß-glucosidase. The spectra are measured for 2, 4, 6, 10, 15, and 30 min after beginning the hydrolysis.

Table 1. Fluorescent properties of flavonols' aglycone and glucoside in dichloromethane.

Flavonol	Fluorescent band maxima, nm (cm^{-1})	
	N* form	T* form
Flavonol glucoside **3a** (*before hydrolysis*)	–	–
Flavonol aglycone **1a** (*after hydrolysis*)	443 (22575)	524 (19085)
Flavonol glucoside **3b** (*before hydrolysis*)	417 (23980)	–
Flavonol aglycone **1b** (*after hydrolysis*)	413 (24215)	532 (18800)

and following extraction can prove the presence of the ß-glucosidase activity.

The results of enzyme activity screening using glucoside **3a**, according to the hydrolysis procedure described in the Experimental part, are depicted in Figure 2. It can be seen that during the hydrolysis reaction between **3a** and ß-glucosidase, the fluorescence intensity of the phototautomer increases that evidences the formation of the aglycone T* form. A weak fluorescence of the form N* seen at 425 nm becomes detectable after 10-30 min of the hydrolysis, under high concentrations of **1a** in organic phase. Spectral characteristics of the corresponding aglycone and flavonol glucosides are summarized in Table 1.

Our above calibration experiment shows that the glucoside of unsubstituted flavonol **3a** can be used as a fluorescent indicator signaling the presence of ß-glucosidase activity; however, quantitative estimation of the absolute activity requires the use of an additional fluorescent standard [26-27].

The fluorescent properties of 4'-benzyloxyflavonol aglycone **1b** and its glucoside **3b** differ from those of **1a** and **3a**. On the one hand, the presence of an electron-donating benzyloxy group in *para*-position to a chromone moiety in **1b** leads to a decrease in the acidity of 3-hydroxy group in the electronic excited-state and, consequently, to a decrease of the ESIPT rate. On the other hand, the presence of the electron-donating substituent leads to a decrease in the energy of the lowest ππ* state relative to the energy of nπ* state, so that it increases the energy gap between these states, and thus, a decrease in intersystem crossing efficiency. Both these effects result in a substantial growth of the fluorescence intensity of the form N* of **1b** relative to that of the N* form of **1a**. Since the lack of ESIPT in protic media, fluorescence spectra of aqueous solutions of **1b** have only one short-wavelength band of the N* form. In non-protic media, spectra of **1b** demonstrate both N* and T* emission bands.

4'-Benzyloxyflavonol glucoside **3b** has a single-band fluorescence spectra in all the media

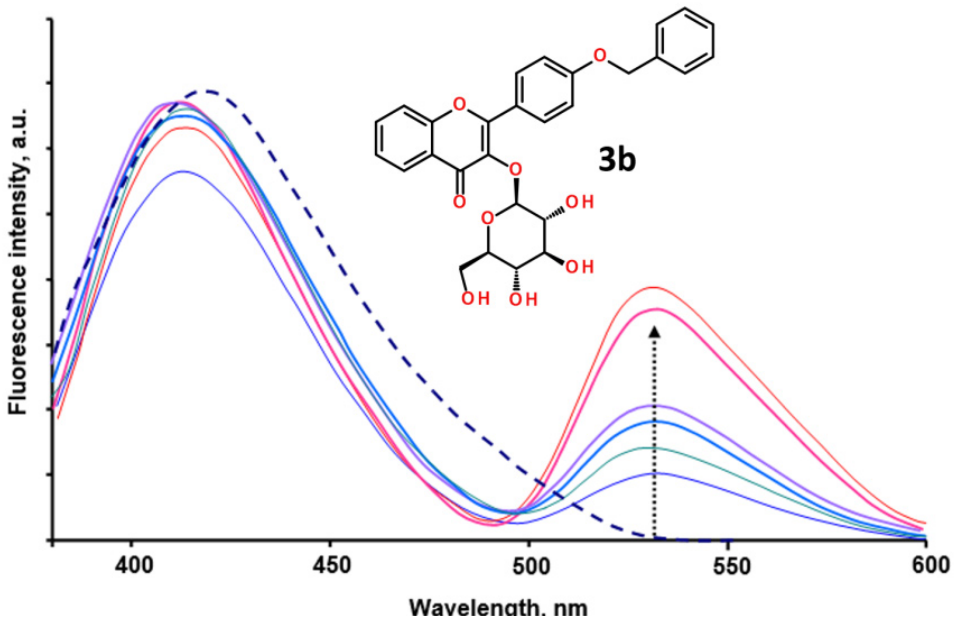

Fig. 3. Changes of fluorescent spectra during the hydrolysis reaction in the system probe **3b** – ß-glucosidase. The spectra are measured for 2, 4, 6, 10, 15, and 30 min after beginning the hydrolysis. Dashed line – the fluorescence spectrum of probe **3b** the organic phase.

due to the emission of the N* form. The spectrum of **3b** in the organic phase is depicted in Figure 3 by a dashed line.

The time evolution of hydrolysis in the reaction between **3b** and ß-glucosidase is shown in Figure 3. The fluorescence spectra registered in the dichloromethane solutions obtained by extraction of aliquots, which were sampled in different time intervals after the beginning of the reaction, showed the presence of the two emission bands. An increase in the intensity of the long-wavelength band T* with reaction time indicates the progress of the formation of aglycone **1b**, evidencing the ß-glucosidase activity. However, it is worth to note the constant intensity of short-wavelength emission band, which is sum of emission bands of the glucoside **3b** and the N* form of **1b** (Figure 3). If one assumes that glucoside **3b** and the N* form of aglycone **1b** have similar quantum yields (due to the similar structure of the fluorophore), it becomes clear that the total intensity of the short-wavelength band does not noticeably change when the ratio of glycoside to aglycone changes during hydrolysis.

The presence of the short-wavelength band with constant intensity seen in Figure 3 allows one to use this band as an internal fluorescent standard. This makes it possible to use the glucoside of 4'-benzyloxy flavonol **3b** not only for detecting the ß-glucosidase activity in biological samples, but also for quantitative estimating this activity.

Kinetics of enzymatic hydrolysis of flavonol glucosides

The kinetics studies of the hydrolysis reaction have been made using fluorescence intensity values in the maxima of the T* bands of aglycones **1a** and **1b**. The analysis of the relationship between T* fluorescence intensity and the time of the reaction was performed using equations describing kinetic reactions of first and second order (Eq. 1-2):

$$\ln C_{glucoside,t} = \ln C_{glucoside,0} - K_{hydr}t \qquad (1)$$

$$\frac{1}{C_{glucoside,t}} = \frac{1}{C_{glucoside,0}} + K_{hydr}t \qquad (2)$$

It was shown that the fluorescence intensities corresponding to the reciprocal values of glycoside concentrations demonstrate a linear dependence on the reaction time (Eq. 2), which corresponds to the 2nd order reaction. Plots of dependencies of reciprocal glucoside concentrations on the reaction time for **3a** and **3b** are depicted in Figure 4.

The rate constants of hydrolysis reactions for **3a** and **3b**, obtained from the analysis of the linear mentioned dependencies, were found to be 81.5 $l \cdot mol^{-1}s^{-1}$ and 35.2 $l \cdot mol^{-1}s^{-1}$, respectively. Thus, it is possible to conclude that the addition of the electron-donating substituent at the 4'-position of flavonol leads to a 2.3-fold decrease in its sensibility to ß-glucosidase actions. It can be explained by the fact that a donor of electronic density in the *para*-position relative

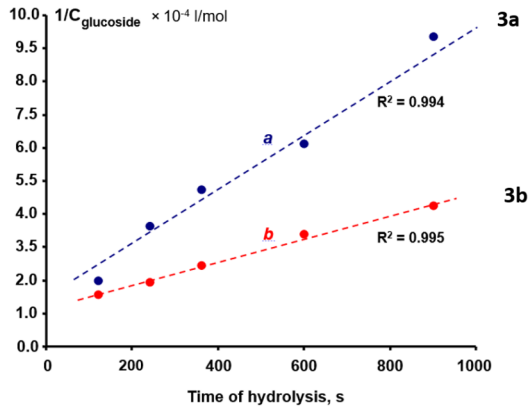

Fig. 4. Kinetics plots for the 2nd order hydrolysis reaction estimated by Eq. 2 for: *a* – probe **3a**, *b* – probe **3b**.

to the chromone moiety increases the negative charge on the oxygen atom at position 3. These electronic effects, in turn, strengthen the chemical bond between the flavonol and the glucoside fragment, thus increasing the stability of the flavonol glucoside with respect to enzyme action.

The fact that enzymatic hydrolysis is a second-order reaction indicates that the rate-limiting step in this process is the binding of flavonol glucosides **3a-b** by ß-glucosidase, rather than the enzymatic cleavage of the O-glycosidic bond in flavonol, releasing corresponding flavonol aglycone and free glucose.

Molecular docking of flavonols against ß-glucosidase

ß-Glucosidases are enzymes, which are widely distributed among all sort of living organisms. Their common feature is enzymatic hydrolysis of ß-glycosidic bonds in disaccharides, oligosaccharides or other conjugated saccharides [41].

The high-resolution 3D structure of commercial ß-glucosidase derived from Almonds are currently not available yet. Therefore, to study flavonol-enzyme interactions by using molecular docking calculations, we used the X-ray structure of the ß-glucosidase enzyme from *Paenibacillus polymyxa* (BglB), which represent a common recognition pattern to all bacterial ß-glucosidases [37, 42-45].

The BglB enzyme has a deep hydrophobic pocket with the active site located at the bottom of this pocket (about 16 Å deep) (Figure 5). The active site contains two glutamate residues Glu167 and Glu356 located at close proximity one another (Figure 5). The X-ray structure of

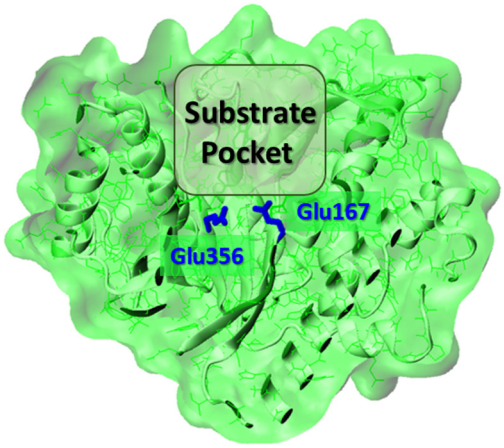

***Paenibacillus polymyxa* β-glucosidase B (BglB)**

Fig. 5. The X-ray structure of *Paenibacillus polymyxa* ß-glucosidase (BglB, PDB ID: 2O9R) [37]. The active site residues Glu167 and Glu356 are shown by blue sticks.

Table 2. The binding affinity of flavonol aglycones **1a-b** and their glucosides **3a-b** towards the ß-glucosidase BglB (PDB: 2O9R).

Ligand	Binding affinity, kcal/mol
1a	-8.2
1b	-9.0
3a	-9.9
3b	-10.8

the ß-glucosidase BglB (PDB 2O9R) [37] was used as a receptor for molecular docking calculations.

Our recent molecular docking studies demonstrated that the binding affinity towards the ß-glucosidase protein depended on the nature of substituents located in a flavonol core [40]. The molecular docking of flavonol aglycones **1a-b** and their glucosides **3a-b** against the ß-glucosidase BglB showed that all the studied probes bind into a central cavity of the enzyme. We found that the binding affinity of probes **1a-b** and **3a-b** depends on their structure and varies in a range from -8.2 up to -10.8 kcal/mol (Table 2). Introducing a bulky hydrophobic benzyloxy moiety in the 4'-aryl ring increases the affinity of probe **3b** towards the ß-glucosidase enzymes compared to flavonol **1a** and its glucoside.

Figure 6 shows the binding mode of flavonol glucosides **3a-b** to the ß-glucosidase BglB estimated by the molecular docking calculations. The ligand-receptor docking suggests that both

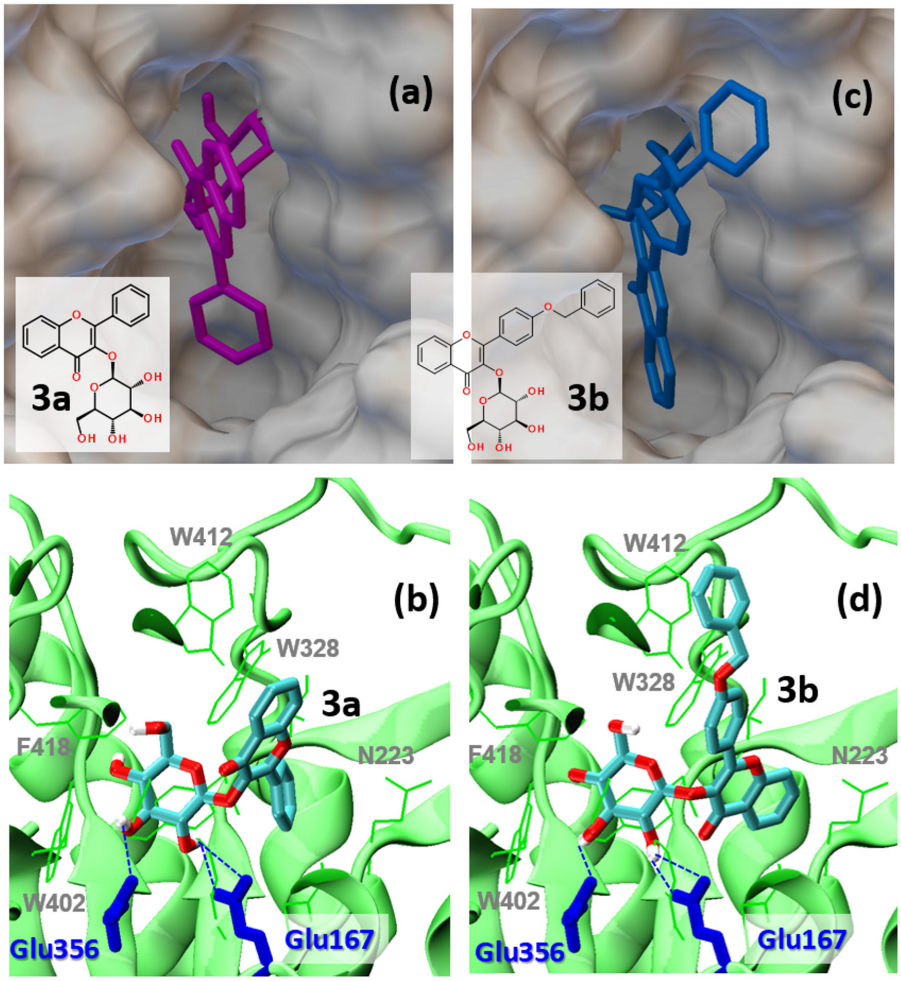

Fig. 6. The best binding mode of flavonol glucosides **3a** (a-b) and **3b** (c-d) to *Paenibacillus polymyxa* ß-glucosidase B (BglB) (PDB code 2O9R) estimated by molecular docking calculations. The enzyme is shown by vdW surface representation for a top view (a, c) and a ribbon model for a side view (b, d), respectively. The probe molecules **3a** and **3b** are shown by a licorice model. The catalytic dyad Glu167-Glu356 of the ß-glucosidase receptor are shown in blue.

flavonol derivatives insert deeply into the hydrophobic cavity of BglB, as seen in Figures 6a and 6c. In the both cases, a D-glucopyranosyl moiety was located in the catalytic sub-pocket in the close proximity to the catalytic dyad Glu167-Glu356, as evident from Figures 6b and 6d. The probe binding to the enzyme is primary driven by hydrophobic interactions with tryptophan aromatic side-chains of W328, W402, W412, as well as with the aromatic ring of F412, respectively.

Figures 6b and 6d show that despite the structure modification in probes **3a-b**, the binding mode of their glucopyranosyl moiety within the active site pocket of the BglB enzyme was found to be similar in many aspects. In both probes **3a** and **3b**, the glucopyranosyl moiety inserts deeply into the catalytic pocket, so that its hydroxyl groups form hydrogen bonds (H-bond) with carboxyl oxygen atoms of the catalytic dyad Glu167-Glu356.

In-depth analysis of the binding interactions of flavonol glucoside **3b** with the BglB enzyme revealed that the bulky 4`-benzyloxy group could not be accommodated within the catalytic pocket of the enzyme, so that it was faced outwards from the catalytic dyad (Figures 6d and 7a). However, it should also be noted that such binding conformation was stabilized by π-π stacking interactions with the tryptophan side-chains of W412 residue. It has been reported that π-π stacking can be considered non-negligible force for stabilizing protein folding and supra-molecular assembly [46]. Figure 7b shows that the contribution of these π-π stacking interactions may be essential forces for stabilizing the bound conformation of probe **3b** within the enzyme pocket. The π-π stacking interactions between the aromatic benzyl and W412 rings are characterized by

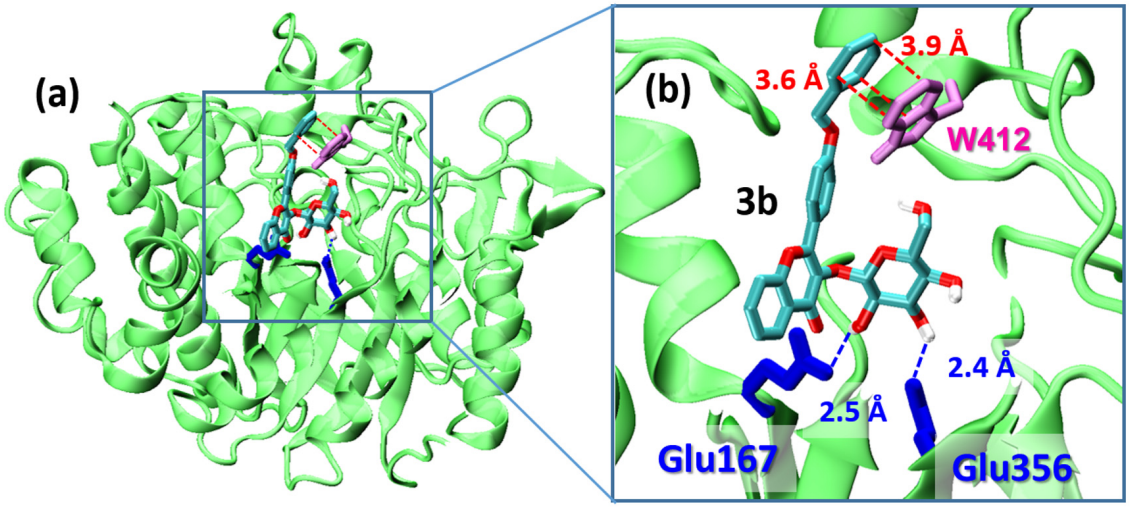

Fig. 7. (**a**) The structure of the enzyme-substrate complex for flavonol glucoside **3b** and the BglB enzyme estimated by molecular docking calculations. (**b**) The insert shows the bound conformation of **3b** in the active site pocket of the BglB enzyme, in which the ligand molecule forms multiple short-range contacts with the enzyme side-chains, such as H-bonds and π-π stacking, shown by dotted lines.

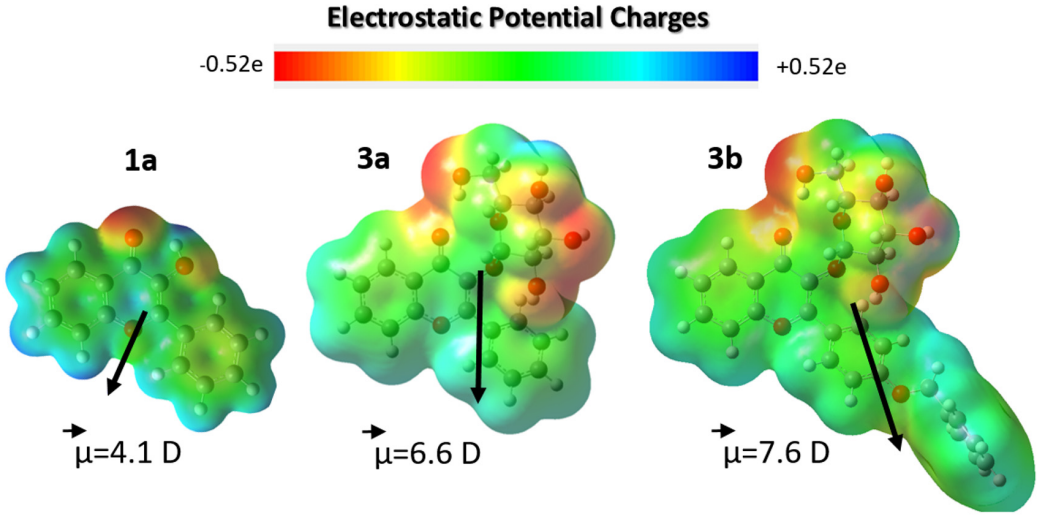

Fig. 8. Electrostatic potential (ESP) maps for probes **1a,** and **3a-b**, calculated at the B3LYP/cc-pVDZ level. A ground-state dipole moment is shown as a vector and its absolute value is given in Debye (D).

short contacts of 3.6-3.9 Å. In combination with H-bonding between the glucopyranosyl moiety and the catalytic dyad, these interactions can explain the intrinsic nature of the tighter binding of flavonol glucoside **3b** to the BglB enzyme. On the other hand, this tight binding mode and additional π-π stacking interactions between probe **3b** and the BglB enzyme would require a higher activation energy barrier to form an appropriate substrate-receptor transition state for the hydrolysis reaction catalyzed by an enzyme-substrate complex.

Among many factors governing the protein-ligand binding, electrostatic binding complementarity and selectivity play a critical role [47]. According to this principle, the optimal receptor-substrate binding occurs at hot spots upon optimal matching between electrostatic potential maps of a catalytic pocket and a substrate [48]. With this goal, we calculated an electrostatic potential (ESP) surface for flavonol glucosides **3a-b** and flavonol aglycone **1a** by the DFT method, as shown in Figure 8. One can notice significant charge alterations within a polar glycopyranosyl moiety of probes **3a-b**, which could govern its electrostatic interactions with charged glutamine carboxyl groups and orient this moiety towards the catalytic dyad Glu167-Glu356 (Figures 6b and 6d).

4. Summary and perspectives

In summary, the application of benzyloxy-substituted flavonol ß-D-glucoside as a fluorescent indicator for the activity screening of the ß-glucosidase enzyme in an aqueous solution was described. The comparison of the rate constant of the enzymatic cleavage of the O-glycosidic bond in benzyloxy-substituted and un-substituted flavonol indicators, estimated by fluorescence kinetic measurements, demonstrated that the introduction of a hydrophobic bulky benzyloxy group in the 4`-position of flavonol resulted in a 2.3-fold decrease of the rate constant of hydrolysis. To shed light on molecular aspects of flavonol-enzyme interactions, the structure of the enzyme-substrate complex was studied by molecular docking calculations. The docking calculations suggest that the probe binding to the enzyme is primarily driven by hydrophobic interactions with tryptophan aromatic side chains of W328, W402, and W412, as well as with the aromatic ring of F412, respectively. The binding affinity of the flavonols towards the ß-glucosidase protein depends on its structure, so that adding a 4`-benzyloxy group to flavonol-glucoside increased the binding affinity from -9.9 to -10.8 kcal/mole. However, the stronger binding of the benzyloxy-substituted glucoside compared to its un-substituted analog would require a higher activation energy barrier to form an appropriate substrate-receptor transition state for the enzymatic hydrolysis reaction, observed as the 2.3-fold decrease in the corresponding rate constant. Finally, these findings open up the opportunity for applying flavonol glucosides as easy-to-use indicators for rapid fluorescent monitoring of other enzyme activity from a glucosidase family [49] .

Acknowledgments: D.O.T., A.Y.C., O.O.K, E.S.G., A.V.K., A.D.R. acknowledge Grant 2020.02/0016 “Indicators based on chromone derivatives for fluorescent determination of ß-glucosidase activity” from the National Research Foundation of Ukraine.

References

1. I. E. Serdiuk, A. D. Roshal. *Dyes and Pigments* **138**, 223-244 (2017). doi: 10.1016/j.dyepig.2016.11.028.
2. A. S. Klymchenko. *Acc. Chem. Res.* **50**, 366-375 (2017). doi: 10.1021/acs.accounts.6b00517.
3. S. Höfener, P. C. Kooijman, J. Groen, F. Ariese, L. Visscher. *Phys. Chem. Chem. Phys.* **15**, 12572-12581 (2013). doi: 10.1039/C3CP44267E.
4. A. Y. Chumak, V. O. Mudrak, V. M. Kotlyar, A. O. Doroshenko. *J. Photochem. Photobiol. A* **406**, 112978 (2021). doi: 10.1016/j.jphotochem.2020.112978.
5. Z. Xu, X. Zhao, M. Zhou, Z. Zhang, T. Qin, D. Wang, L. Wang, X. Peng, B. Liu. *Sens. Actuators, B* **345**, 130367 (2021). doi: 10.1016/j.snb.2021.130367.
6. T. Qin, B. Liu, Y. Huang, K. Yang, K. Zhu, Z. Luo, C. Pan, L. Wang. *Sens. Actuators, B* **277**, 484-491 (2018). doi: 10.1016/j.snb.2018.09.056.
7. T. Qin, B. Liu, Z. Xu, G. Yao, H. Xu, C. Zhao. *Sens. Actuators, B* **336**, 129718 (2021). doi: 10.1016/j.snb.2021.129718.
8. A.D. Roshal. *Chem. Record*, e202300249 (2023). doi: 10.1002/tcr.202300249.
9. A. Kyrychenko, A. S. Ladokhin. *Chem. Record*, e202300232 (2023). doi: 10.1002/tcr.202300232.
10. X. Bi, B. Liu, L. McDonald, Y. Pang. *J. Phys. Chem. B* **121**, 4981-4986 (2017). doi: 10.1021/acs.jpcb.7b01885.
11. D. McMorrow, M. Kasha. *J. Phys. Chem.* **88**, 2235-2243 (1984). doi: 10.1021/j150655a012.
12. A. D. Roshal, J. A. Organero, A. Douhal. *Chem. Phys. Lett.* **379**, 53-59 (2003). doi: 10.1016/j.cplett.2003.08.008.
13. I. E. Serdiuk, A. D. Roshal. *RSC Adv.* **5**, 102191-102203 (2015). doi: 10.1039/C5RA13912K.
14. A. O. Doroshenko, A. V. Kyrychenko, O. M. Valyashko, V. N. Kotlyar, D. A. Svechkarev. *J. Photochem. Photobiol. A* **383**, art. no. 111964 (2019). doi: 10.1016/j.jphotochem.2019.111964.
15. A. P. Demchenko, S. Ercelen, A. D. Roshal, A. S. Klymchenko. *Polish J. Chem.* **76**, 1287-1299 (2002).
16. V. F. Valuk, G. Duportail, V. G. Pivovarenko. *J. Photochem. Photobiol. A* **175**, 226-231 (2005). doi: 10.1016/j.jphotochem.2005.05.003.
17. X. Poteau, G. Saroja, C. Spies, R. G. Brown. *J. Photochem. Photobiol. A* **162**, 431-439 (2004). doi: 10.1016/s1010-6030(03)00429-5.
18. W. Liu, Y. Wang, W. Jin, G. Shen, R. Yu. *Analyt. Chim. Acta* **383**, 299-307 (1999). doi: 10.1016/s0003-2670(98)00789-2.
19. X. Jin, X. Sun, X. Di, X. Zhang, H. Huang, J. Liu, P. Ji, H. Zhu. *Sens. Actuators, B* **224**, 209-216 (2016). doi: 10.1016/j.snb.2015.09.072.
20. A. D. Roshal, A. V. Grigorovich, A. O. Doroshenko, V. G. Pivovarenko, A. P. Demchenko. *J. Phys. Chem. A* **102**, 5907-5914 (1998). doi: 10.1021/jp972519w.
21. A. D. Roshal, T. V. Sakhno, A. A. Verezubova, L. M. Ptiagina, V. I. Musatov, A. Wroblewska, J. Blazejowski. *Funct. Mater.* **10**, 419-426 (2003).

22. A. Munoz, A. D. Roshal, S. Richelme, E. Leroy, C. Claparols, A. V. Grigorovich, V. G. Pivovarenko. *Russ. J. Gen. Chem.* **74**, 438-445 (2004). doi: 10.1023/B:RUGC.0000030403.41976.5c.
23. B. Liu, Y. Pang, R. Bouhenni, E. Duah, S. Paruchuri, L. McDonald. *Chem. Commun.* **51**, 11060-11063 (2015). doi: 10.1039/C5CC03516C.
24. K. A. Bertman, C. S. Abeywickrama, H. J. Baumann, N. Alexander, L. McDonald, L. P. Shriver, M. Konopka, Y. Pang. *J. Mater. Chem. B* **6**, 5050-5058 (2018). doi: 10.1039/C8TB00325D.
25. K. A. Bertman, C. S. Abeywickrama, A. Ingle, L. P. Shriver, M. Konopka, Y. Pang. *J. Fluoresc.* **29**, 599-607 (2019). doi: 10.1007/s10895-019-02371-7.
26. I. E. Serdiuk, M. Reszka, H. Myszka, K. Krzymiński, B. Liberek, A. D. Roshal. *RSC Adv.* **6**, 42532-42536 (2016). doi: 10.1039/C6RA06062E.
27. M. Reszka, I. E. Serdiuk, K. Kozakiewicz, A. Nowacki, H. Myszka, P. Bojarski, B. Liberek. *Org. Biomol. Chem.* **18**, 7635-7648 (2020). doi: 10.1039/D0OB01505A.
28. A. T. Adetunji, F. B. Lewu, R. Mulidzi, B. Ncube. *J. Soil Plant Nutr.* **17**, 794-807 (2017). doi: 10.4067/S0718-95162017000300018.
29. L. L. Escamilla-Treviño, W. Chen, M. L. Card, M.-C. Shih, C.-L. Cheng, J. E. Poulton. *Phytochem.* **67**, 1651-1660 (2006). doi: 10.1016/j.phytochem.2006.05.022.
30. A. V. Morant, K. Jørgensen, C. Jørgensen, S. M. Paquette, R. Sánchez-Pérez, B. L. Møller, S. Bak. *Phytochem.* **69**, 1795-1813 (2008). doi: 10.1016/j.phytochem.2008.03.006.
31. T. D. Butters. *Curr Opin Struct Biol* **11**, 412-418 (2007). doi: 10.1016/j.cbpa.2007.05.035.
32. X. Zhou, Z. Huang, H. Yang, Y. Jiang, W. Wei, Q. Li, Q. Mo, J. Liu. *Biomed Pharmacotherapy* **91**, 504-509 (2017). doi: 10.1016/j.biopha.2017.04.113.
33. Z. Qiang, W. Chun, L. Yunping, P. Wenchen. *Chin. J. Appl. Environ. Biol.* **23**, 232-237 (2017). doi: 10.3724/SP.J.1145.2016.04019.
34. R. S. Khodzhaieva, E. S. Gladkov, A. Kyrychenko, A. D. Roshal. *Front. Chem.* **9**, 637944 (2021). doi: 10.3389/fchem.2021.637994.
35. D. S. Goodsell, G. M. Morris, A. J. Olson. *J. Mol. Recognit.* **9**, 1-5 (1996). doi: 10.1002/(SICI)1099-1352(199601)9:1<1::AID-JMR241>3.0.CO;2-6.
36. O. Trott, A. J. Olson. *J. Comput. Chem.* **31**, 455-461 (2010). doi: 10.1002/jcc.21334.
37. P. Isorna, J. Polaina, L. Latorre-García, F. J. Cañada, B. González, J. Sanz-Aparicio. *J. Mol. Biol.* **371**, 1204-1218 (2007). doi: 10.1016/j.jmb.2007.05.082.
38. W. Humphrey, A. Dalke, K. Schulten. *J. Mol. Graphics* **14**, 33-38 (1996). doi: 10.1016/0263-7855(96)00018-5.
39. V. G. Pivovarenko. *BBA Adv.* **3**, 100094 (2023). doi: 10.1016/j.bbadva.2023.100094.
40. O. O. Demidov, E. S. Gladkov, A. V. Kyrychenko, A. D. Roshal. *Funct. Mater.* **29**, 252-262 (2022). doi: 10.15407/fm29.02.252.
41. Y. Bhatia, S. Mishra, V. S. Bisaria. *Crit. Rev. Biotech.* **22**, 375-407 (2002). doi: 10.1080/07388550290789568.
42. S. Tribolo, J.-G. Berrin, P. A. Kroon, M. Czjzek, N. Juge. *J. Mol. Biol.* **370**, 964-975 (2007). doi: 10.1016/j.jmb.2007.05.034.
43. S. He, S. G. Withers. *J. Biol. Chem.* **272**, 24864-24867 (1997). doi: 10.1074/jbc.272.40.24864.
44. J. R. Ketudat Cairns, B. Mahong, S. Baiya, J.-S. Jeon. *Plant Sci.* **241**, 246-259 (2015). doi: 10.1016/j.plantsci.2015.10.014.
45. A. D. Snizhko, A. V. Kyrychenko, E. S. Gladkov. *Int. J. Mol. Sci.* **23**, 3781 (2022). doi: 10.3390/ijms23073781.
46. J.-H. Deng, J. Luo, Y.-L. Mao, S. Lai, Y.-N. Gong, D.-C. Zhong, T.-B. Lu. *Sci. Adv.* **6**, eaax9976 (2020). doi: 10.1126/sciadv.aax9976.
47. S. Y. Willow, B. Xie, J. Lawrence, R. S. Eisenberg, D. D. L. Minh. *Phys. Chem. Chem. Phys.* **22**, 12044-12057 (2020). doi: 10.1039/D0CP00376J.
48. T. Sulea, E. O. Purisima. *Biophys. J.* **84**, 2883-2896 (2003). doi: 10.1016/S0006-3495(03)70016-2.
49. L. V. Chepeleva, O. O. Demidov, A. D. Snizhko, D. O. Tarasenko, A. Y. Chumak, O. O. Kolomoitsev, V. M. Kotliar, E. S. Gladkov, A. Kyrychenko, A. D. Roshal. RSC Adv. 13, 34107-34121 (2023). doi:10.1039/D3RA06276G.